A R C H I V E S O F M E T A L L U R G Y A N D M A T E R I A L S
Volume 60 2015 Issue 1
DOI: 10.1515/amm-2015-0031

P. ZYGOŃ*, M. GWOŹDZIK*, J. PESZKE**, Z. NITKIEWICZ*

COMPARISON OF PROPERTIES OF POLYMER COMPOSITE MATERIALS REINFORCED WITH CARBON NANOTUBES

PORÓWNANIE WŁAŚCIWOŚCI KOMPOZYTÓW POLIMEROWYCH WZMACNIANYCH NANORURKAMI WĘGLOWYMI

Carbon nanotubes because of their high mechanical, optical or electrical properties, have found use as semiconducting materials constituting the reinforcing phase in composite materials. The paper presents the results of the studies on the mechanical properties of polymer composites reinforced with carbon nanotubes (CNT). Three-point bending tests were carried out on the composites. The density of each obtained composite was determined as well as the surface roughness and the resistivity at room temperature.

Moreover the surface studies on an atomic forces microscope (AFM) and X-ray studies (phase composition analysis, crystallite sizes determination) were carried out on such composites. Measurements of the surface topography using the Tapping Mode method were performed, acquiring the data on the height and on the phase imaging. The change of intensity, of crystallite size and of half-value width of main reflections originating from carbon for composites have been determined using the X-ray analysis.

Carbon nanotubes constituting the reinforcement for a polymer composite improve the mechanical properties and conductivity of the composite.

Keywords: carbon nanotubes, AFM, surface topography, polymer composites, mechanical

Nanorurki węglowe ze względu na wysokie właściwości mechaniczne, optyczne czy elektryczne znalazły zastosowanie jako faza wzmacniająca materiałów kompozytowych. W pracy przedstawiono wyniki badań właściwości mechanicznych kompozytów polimerowych wzmacnianych nanorurkami węglowymi (CNT). Na kompozytach została przeprowadzona próba trójpunktowego zginania. Określono gęstość każdego z otrzymanych kompozytów, wyznaczono chropowatość powierzchni na profilometrze oraz rezystywność w temperaturze pokojowej.

Dla każdego z kompozytów przeprowadzono również badania powierzchni na mikroskopie sił atomowych (AFM), badania rentgenograficzne (analiza składu fazowego, określenie wielkości krystalitów). Przeprowadzono pomiary topografii powierzchni metodą Tapping Mode zbierając dane z wysokości i obrazowania fazowego. Za pomocą analizy rentgenograficznej określono zmianę intensywności, wielkości krystalitów oraz szerokości połówkowej refleksów głównych pochodzących od węgla dla nanorurek różnie modyfikowanych.

Nanorurki węglowe stanowiące zbrojenie dla kompozytów polimerowych poprawiają właściwości mechaniczne oraz przewodność kompozytu.

1. Introduction

Discovered in the last century and thoroughly characterised by a team headed by Ijiama, in 1991, carbon nanotubes (CNT) arose a great interest in the application of nanometric structures in numerous branches of research and industry [1]. CNTs belong to the group of so-called nanomaterials, which feature unique physical properties, resulting directly from their structure of nanometric dimensions [2]. They have extremely high mechanical properties: the tensile strength up to Rm ≅ 500 GPa, and the modulus of elasticity reaches E ≅ 7-8 TPa [3]. They are produced using such techniques as: an electric arc method, a catalytic laser synthesis and various types of chemical vapours deposition (CVD) [4].

Theoretical predictions show that carbon nanotubes behave as either metals or semiconductors, depending on their diameters and degrees of chirality. Each nanotube is unique when it is considered as a nanowire of nanometer scale, but it is unnecessary to know the properties of each nanotube when it is used in an ensemble as an engineering material. It is of great interest to investigate the behavior of nanotubes on a macroscopic scale [5].

Carbon nanotubes may be classified as single-walled carbon nanotubes (SWNTs), double-walled carbon nanotubes (DWNTs) or multi-walled carbon nanotubes (MWNTs) [6]. SWNT and DWNT comprise cylinders of one or two (concentric), respectively, graphene sheets, whereas MWNT consists several concentric cylindrical shells of graphene sheets [7].

* CZESTOCHOWA UNIVERSITY OF TECHNOLOGY, INSTITUTE OF MATERIALS ENGINEERING, 19 ARMII KRAJOWEJ AV., 42-201 CZĘSTOCHOWA, POLAND
** UNIVERSITY OF SILESIA IN KATOWICE, DEPARTMENT OF SOLID STATE PHYSICS, 4 UNIWERSYTECKA STR., 40-007 KATOWICE, POLAND

To obtain nanocomposites with CNTs the following parameters are critical: good CNTs dispersion in the matrix, their good wetting by the polymer, a high adhesion on the phase boundary. It is not easy to satisfy these requirements [8]. Individual CNTs join forming multi-fibrous bands (ropes, bundles), bound by van der Waals forces, and these continue aggregating [9]. Because of these excellent properties, CNTs can be used as ideal reinforcing agents for high performance polymer composites. Ajayan et al. [10] reported the first polymer nanocomposites using CNTs as a filler. The number of articles and patents in polymer composites containing CNTs is increasing every year [11]. Various polymer matrices are used for composites, including thermoplastics, thermosetting resins, liquid crystalline polymers, water-soluble polymers, conjugated polymers, among others. The properties of polymer composites that can be improved due to presence of CNTs include tensile strength, tensile modulus, toughness, glass transition temperature, thermal conductivity, electrical conductivity, solvent resistance, optical properties, etc. [7].

It is believed that the inclusion of carbon nanotubes to the polymer matrix will result in development of many advanced properties of composite materials [12]. Carbon nanotubes are widely used in various areas of science and industry. Most of the applications focus around their electric and mechanical properties.

2. Material and experimental methods

CNT CO. LTD carbon nanotubes, with a commercial name C_{TUBE} 100, obtained using the thermal CVD method and polyvinyl alcohol with a water acrylate dispersion were used as the studied material. Raw nanotubes were 1 to 25 μm long, 10 to 40 nm in diameter, with the density of 0.03-0.06 g/cm^3 and the specific surface area of 150-250 m^2/g. Polyvinyl alcohol (PVA) with a water acrylate dispersion (Osakryl 319M, Oskaryl AZ, Oskaryl OA) was used as the matrix.

Composites were produced using the solvent method, i.e. via mixing in the solution. Carbon nanotubes used for the reinforcement of composites were not pre-treated or modified. The first stage consisted of mixing nanotubes with the polymer and water acrylate dispersion. The solvent was then removed by evaporation. After spontaneous evaporation of the solvent, composites were crosslinked at room temperature during 30 days. Produced composites featured various type of water acrylate dispersion. The composition of the produced composites is presented in Table 1.

TABLE 1
Composition of the produced composites [% wt.]

	CNT	*PVA*	*Water acrylate dispersion*		
			OSA 319M [%]	*OSA AZ [%]*	*OSA OA [%]*
Composite 1	9	73	18	-	-
Composite 2	9	73	-	18	-
Composite 3	9	73	-	-	18

Then test specimens of 10 mm×10 mm×60 mm dimensions were cut for three-point bending. Tests were carried out on ZWICK/ROELL Z100 testing machine using the force of 50 kN.

Roughness was measured on a T600 HOMMEL TESTER, in which the surface shape is mechanically followed by a system of moving inductive converter. Studies of surface topography were performed on a VEECO MULTIMODE atomic forces microscope (AFM) with a NANOSCOPE controller by means of the Tapping Mode method, acquiring the data on the height, amplitude of vibrations and on the phase imaging. The surface studies were carried out in the area of 5 μm×5 μm.

The X-ray phase analysis was carried out using a SEIFERT 3003T/T X-ray diffractometer with a cobalt tube of λ =0.17902 nm wavelength. The X-ray studies were performed comprising measurements at a symmetric Bragg-Brentano geometry (XRD) within the 5 – 120° range of angles with an angular step of 0.1° and the exposure time of 3 seconds. To interpret the results (to determine the 2θ position and the total intensity I_{Net} and the crystallite sizes) the diffractograms were described by a Pseudo Voight curve using the Analyze software. A computer software and the DHN PDS crystallographic database were used for the phase identification.

Each composite density was also measured. The basic method of density measurement consists of independent measurement of specimen mass and volume. Specimens mass was determined by means of an electronic balance (Δ±0.01 g) and the volume of cuboidal specimens via measuring their dimensions using a vernier calliper (Δ±0.01 mm).

Also the resistance of each composite material has been measured. The measurement stand has been equipped with the electrometer Keithley 6417B, which enables taking exact measurements of superficial current Is, as well as certified measurement electrodes. The samples have been subjected to conditioning for 24 hours at the temperature of 22.5°C and relative humidity of 65%.

3. Results of tests

Composite roughness measurements were performed on an area LT = 4.80 mm long with the precision of LC = 0.80 mm. Tests resulted in obtaining graphs for studied composites, where voltage changes were recorded in the form of peaks, evaluated by means of the instrument head electronics, which are converted into a signal proportional to position changes of the diamond tip, by means of which appropriate surface parameters are displayed and documented. Basic parameters of studied material surface roughness include:

– R_a – arithmetical mean roughness deviation,
– R_{max} – maximum roughness height,
– R_t – maximum elevation – cavity height,
– R_z – average roughness height,
– R_p – maximum height of elevation.

The roughness results obtained (Tab. 2, Fig. 1) demonstrated that composite material 2 has been characterised by the highest roughness value. On the other hand, the matrix itself demonstrated the lowest roughness values.

On the roughness diagrams obtained (Fig. 1) one can notice high peaks, which testify about somewhat high roughness of the composite material surface. The highest rough-

ness has been observed for composite material 2, fore which the average roughness parameter amounted to ~17.8 μm. The roughness parameter for the remaining composite materials varies between 12 and 15 μm. The lowest value of roughness parameter has been observed in case of matrix, for which that parameter had the value of ~1μm.

TABLE 2
Basic roughness parameters of studied composites surface

	Matrix	*Composite 1*	*Composite 2*	*Composite 3*
R_a *[μm]*	0.97	12.62	17.79	15.89
R_{max} *[μm]*	7.96	99.24	140.35	93.62
R_t*[μm]*	9.19	99.24	140.35	99.70
R_z*[μm]*	5.08	71.36	88.08	79.20
R_p *[μm]*	5.76	43.73	63.15	49.75

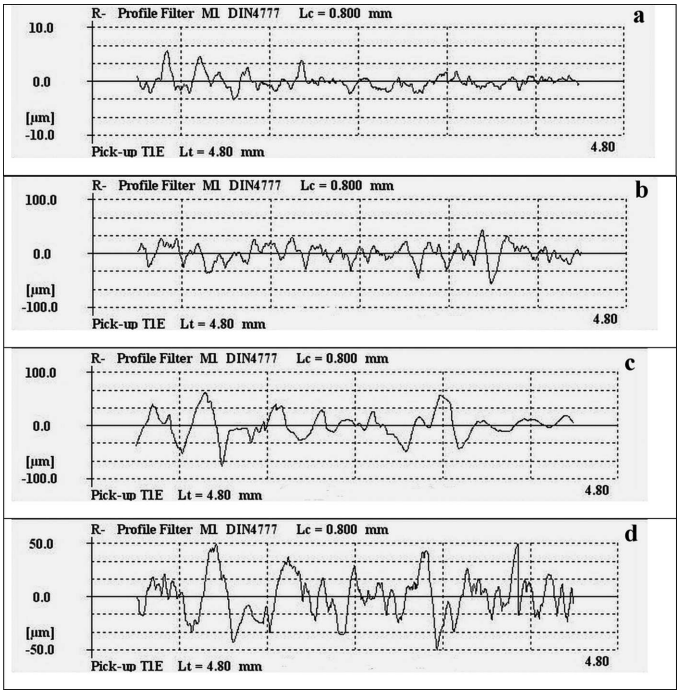

Fig. 1. Roughness measurement graphs for individual composites and matrix: a) matrix; b) composite 1; c) composite 2; c) composite 3

Figure 2a presents the image of surface topography of composite material 1, obtained during examination using atomic force microscope.

Substantial agglomerates of nanotubes are visible on the surface of composite material 1. Their even distribution over the entire surface of the composite material can be noted.

Figure 3a shows the image of the surface of composite material 2, on which a linear distribution of nanotubes in the matrix can be noted. Also, images obtained from amplitude (Fig. 3c) and phase imaging (Fig. 3d) are presented.

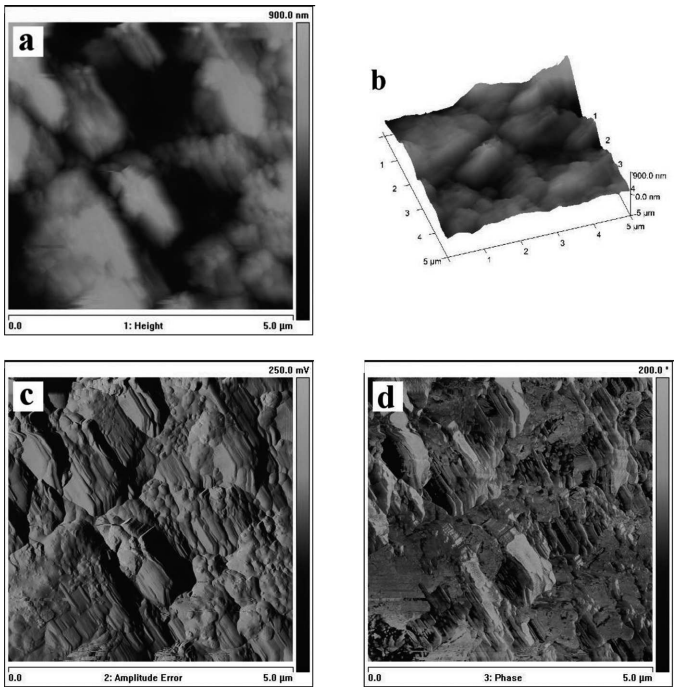

Fig. 2. Surface topography of composite material 1: a) surface topography 2D; b) surface topography 3D; c) amplitude of vibrations; d) phase imaging

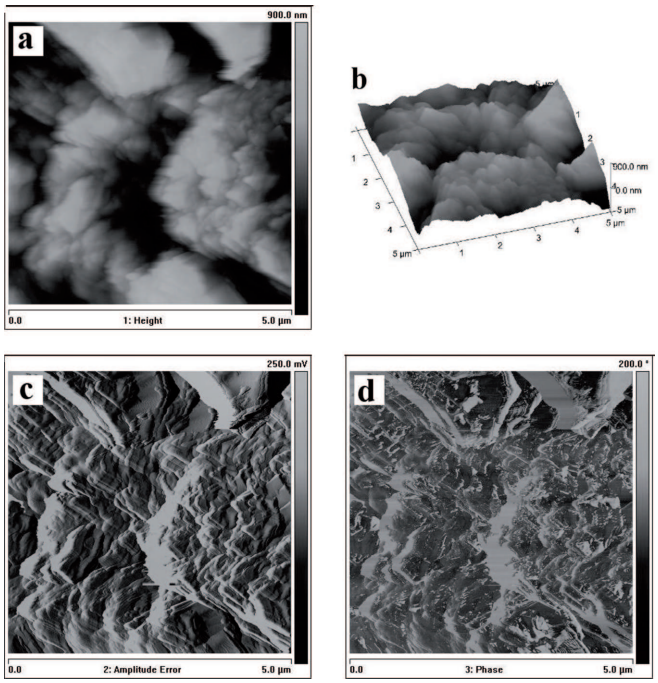

Fig. 3. Surface topography of composite material 2: a) surface topography 2D; b) surface topography 3D; c) amplitude of vibrations; d) phase imaging

On the surface of composite material 3 one can note the distribution of carbon nanotubes in the composite material (Figs. 4a, 4b). Twisted nonotubes can be noted. Nanotubes can be observed very clearly in phase imaging (Fig. 4d). It is possible to see the even distribution of nanotubes over the entire surface of the composite material.

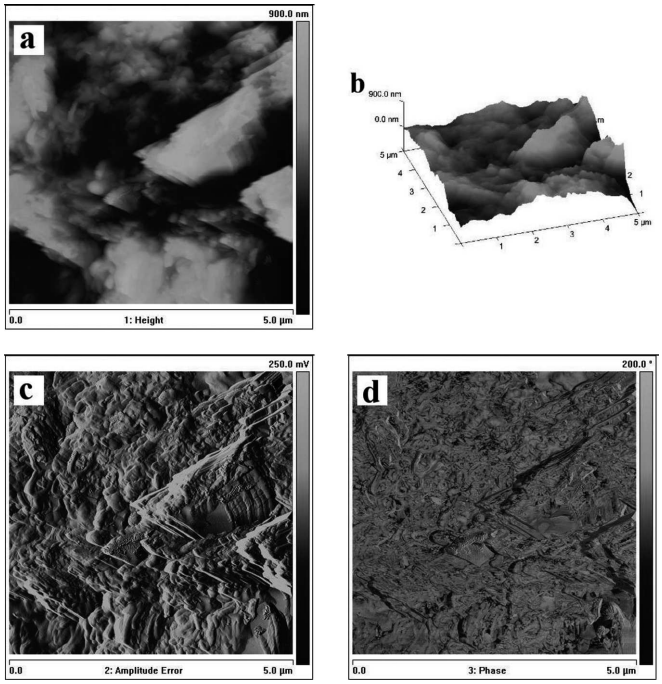

Fig. 4. Surface topography of composite material 3: a) surface topography 2D; b) surface topography 3D; c) amplitude of vibrations; d) phase imaging

Carbon nanotubes are characterised by relatively small diameter, which can be noticed on Figs. 2-4. Raw nanotubes, in the course of mechanical mixing and exposure to ultrasounds have not been thoroughly separated, though, and one can still see agglomerates that still stick together and are twisted.

Measurements of surface topography, amplitude of vibrations, and phase imaging for the matrix have also been carried out. The results of those examinations are presented on Figure 5.

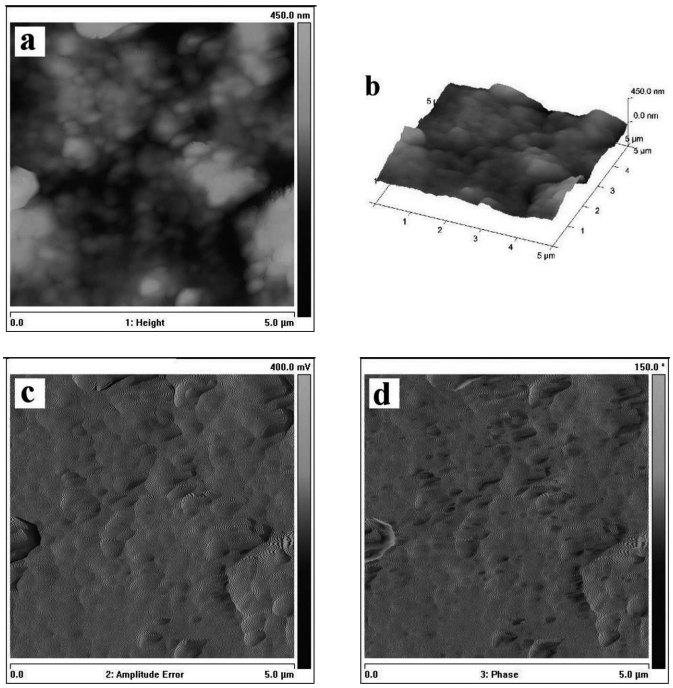

Fig. 5. Surface topography of matrix: a) surface topography 2D; b) surface topography 3D; c) amplitude of vibrations; d) phase imaging

Figure 5a shows the image of matrix surface topography, which is characterised by small bubbles, which got formed during setting of the polymer.

The lowest value of roughness parameter was demonstrated by the matrix, for which the average roughness parameter Ra amounted to ~35 nm, while the maximum roughness value was ~373 nm. Composite materials are characterised by a similar roughness, which varies between 104 and 124 nm (Fig. 6).

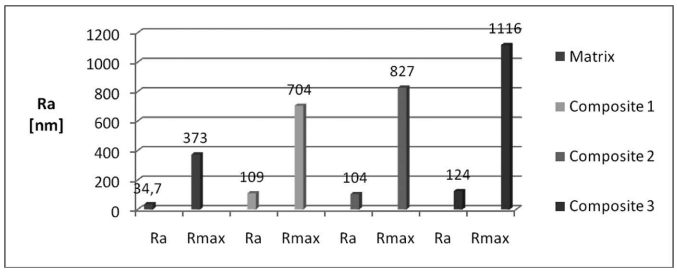

Fig. 6. Avarage arithmetical roughness for individual composites

Roentgenography-derived diffractograms (Fig. 7) show characteristic peaks that are caused by carbon. The peak characteristic for the matrix is derived from carbon from the hydrocarion chain, which is typical for polymers. The hybridisation that occurs between such atoms of carbon is sp^3. On the other hand, the peaks that are visible on diffractograms of composite materials derive from graphite. For such links between carbon atoms the sp^2 hybridisation is characteristic.

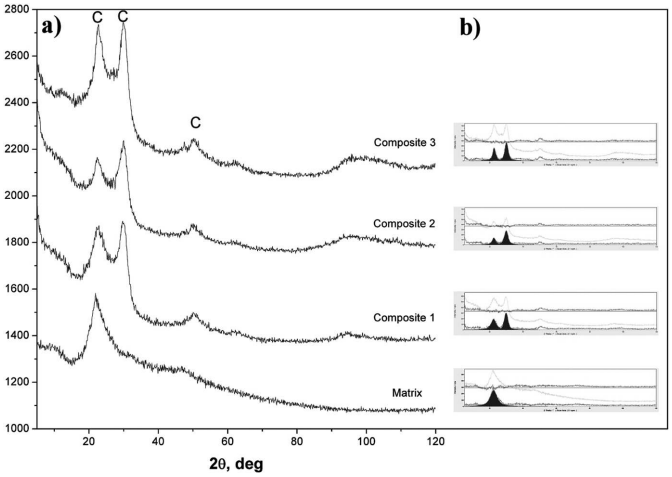

Fig. 7. The X-ray diffractograms of individual composites and matrix (a); fitting by means of the Analyze software (b)

Main reflections from carbon from hydrocarbon chain and graphite from carbon nanotubes have been subjected to more thorough analysis. The total intensity of reflections derived from carbon as well as graphite turned out to be the highest for composite material 3, and the lowest for composite material 2 (Fig. 8).

On the other hand, the total intensity derived from carbon is much higher for the matrix than for composite materials.

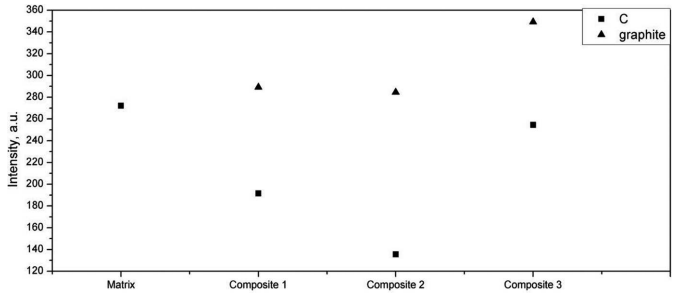

Fig. 8. Total intensity of the main reflection originating from carbon

The most narrow diffraction line has been observed for composite material 3 (Fig. 9), whereas the widest one for composite material 1, which is caused by reduction of crystallite size (Fig. 10).

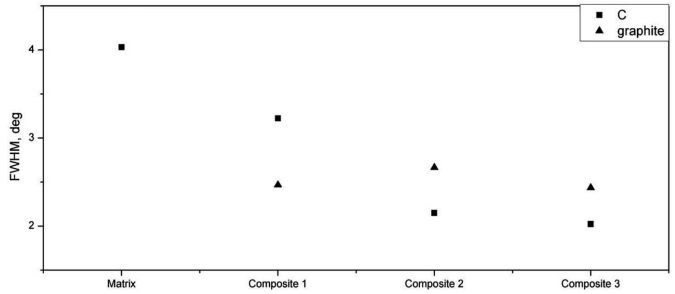

Fig. 9. Half-value width of the main reflection originating from carbon

X-ray examinations performed on composite materials reveal, not only intensity of reflections change, but also their full width at half maximum. As is known, the change in width may result both from a change in the size of crystallites, as well as stresses in the material. Composite material 3 is characterised by having biggest crystallites (Fig. 10) derived both from carbon and graphite, that varies for composite materials 1 and 2. On the other hand, the lowest carbon-derived crystallite size has been observed for the matrix.

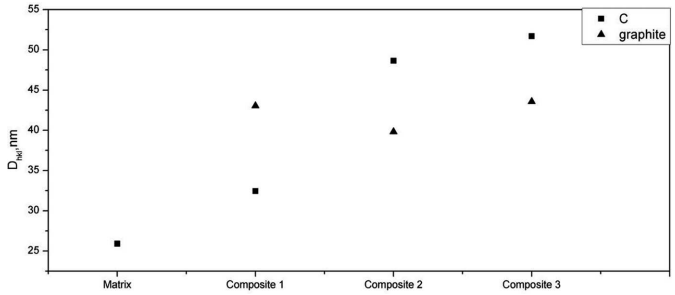

Fig. 10. D_{hkl} crystallite sizes for the main reflection originating from carbon

The results of tests concerning resistivity, flexural strength, and density of composite materials are published in Table 3.

The highest resistivity and density have been observed in the case of composite material 1, containing OSA 319M dispersion. Its density amounted to 0.43 g/cm^3, while its resistivity to 291 Ω·m. The lowest resistivity value has been noted for composite material 3, containing OSA OA dispersion, its resistivity amounted to 177 Ω·m while its density was 0.35 g/cm^3. The lowest density, amounting to 0.28 g/cm^3 was noted for composite material 2, containing OSA OZ dispersion. Its resistivity amounted to 192 Ω·m.

TABLE 3
Metallic radii of rare earth metals and magnesium [12]

	Density d [g/dm^3]	***Bending strength Rg [MPa]***	***Resistivity ρ_s [Ω ·m]***
Matrix	1.22	-	2,84·10^{10}
Composite 1	0.43	6.533	291
Composite 2	0.28	1.068	192
Composite 3	0.35	1.633	177

Figure 11 contains graphs illustrating flexural strength of the composite materials. Unfortunately, the three-point bending test could not be carried out, due to flexibility, and plasticity.

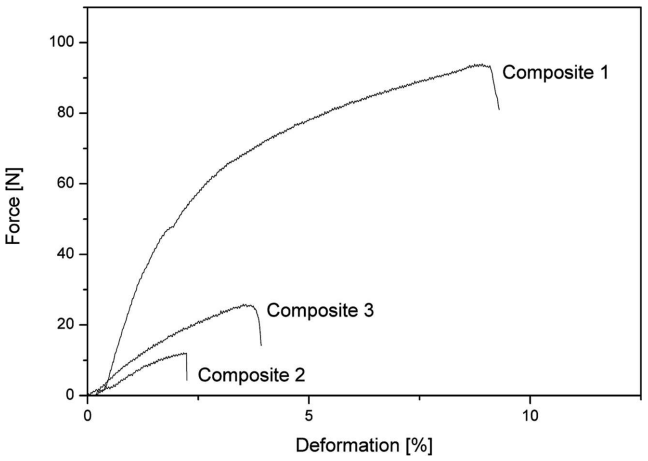

Fig. 11. Force vs. deformation curves obtained from three-point bending test

Graphs provide information about the maximum force used for breaking a sample, on that basis the flexural strength has been determined (Table 3). The highest value of flexural strength has been noted in the case of composite material 1, for which the Rg value amounted to 6.533 MPa. For composite material 3 the flexural strength amounted to 1.633 MPa, whereas composite material 2 revealed the lowest flexural strength. For the latter, the value of Rg was 1.068 MPa.

4. Summary of results

Roughness measurements, performed on profile measuring device on an area greater than that covered by atomic force microscopy demonstrated, that the roughness of composite materials varied between 12-18 μm, while for mere matrix the roughness value amounted to ~1μm. The results of tests performed using a profile meter confirmed the results of roughness measurements performed using atomic force microscope.

The examinations of surface topography, performed by means of atomic force microscopy, revealed that composite materials have similar roughness values, which were of the

104-124 nm range. On the other hand, the matrix is characterised by significantly lower Ra coefficient, amounting to 34.7 nm.

It results from the roentgenographic examinations that the characteristic peak, which has been noted for composite materials is a graphite-derived peak. Also the carbon-derived peak, typical for hydrocarbon chains, is visible.

The density of composite materials varies in the range of 0.28-0.43 g/cm^3, which is satisfactory, as the assumption has been to obtain composite materials with as low density as possible.

The highest strength parameter has been noted for composite material 1, for which Rg amounted to 6.533 MPa, whereas the lowest flexural strength has been noted in case of composite material 2. For the latter, the Rg amounted to 1.068 MPa.

Addition of nanotubes to the matrix results in marked improvement of conductivity of composite materials. The resistivity for matrix alone amounted to $2.84 \cdot 10^{10} \Omega \cdot$m, whereas after addition of nanotubes it varies between 177 and 291 $\Omega \cdot$m. Carbon nanotubes significantly improve the conductivity of composite materials.

The best properties, despite being the most dense one, belonged to composite material 1, which contained the OSA 319M dispersion. It demonstrated the lowest roughness, together with the highest flexural strength and resistivity.

REFERENCES

[1] S. Ijima, Helical microtubules of graphitic carbon. Nature **354**, 56-58 (2001).

[2] G. Zhu, X.P. Zou, J. Cheng, M.F. Wang, Y. Su, Arch. Metall. Mater. **53**, 3, 735-740 (2008).

[3] M. Jakubowska, D. Biało, M. Słoma, A. Młożniak, Nowoczesne materiały kompozytowe zawierające nanorurki węglowe do zastosowań w technologii grubowarstwowej. Kompozyty, 2, 158-163 (2008).

[4] P. Zygoń, M. Gwoździk, J. Peszke, Z. Peszke, Surface topography of carbon nanotubes posing a reinforcing phase in composite materials. Kompozyty, 4, 262-265 (2012).

[5] R.Z. Ma, C.L. Xu, B.Q. Wei, J. Liang, D.H. Wu, D.J. Li, Electrical conductivity and field emission characteristics of hot-pressed sintered carbon nanotubes. Materials Research Bulletin **34**, 5, 741-747 (1999).

[6] A. Huczko, Nanorurki węglowe. Czarne diamenty XXI wieku, Warszawa (2004).

[7] N.G. Sahoo, S. Rana, J.W. Cho, L. Li, S.H. Chan, Polymer nanocomposites based on functionalized carbon nanotubes. Progress in Polymer Science **35**, 837-867 (2010).

[8] P. Zygoń, M. Gwoździk, J. Peszke, Z. Nitkiewicz, C. Kolan, Properties of polimer composites reinforced with carbon nanotubes. Hutnik – Wiadomości Hutnicze, 5, 366-368 (2013).

[9] Z. Rosłaniec, G. Broza, K. Schulte, Nanocomposites based on multiblock polyester elastomers (PEE) and carbon nanotubes (CNT). Composite Interfaces **10**, 1, 95-102 (2003).

[10] P.M. Ajayan, O. Stephan, C. Colliex, D. Trauth, Aligned carbon nanotube arrays formed by cutting a polymer resin-nanotube composite. Science **265**, 1212-1214 (1994).

[11] M. Moniruzzaman, K.I. Winey, Polymer nanocomposites containing carbon nanotubes. Macromolecules **39**, 5194-5205 (2006).

[12] M.S.P. Shaffer, A.H. Windle, Fabrication and characterization of carbon nanotubes/poly(vinyl alcohol) composites. Advanced Materials **11**, 937-941 (1999).

Received: 20 March 2014.